



ARTICLE

Antimicrobial Activity of Substituted Benzopentathiepin-6-amines

Tatyana M. Khomenko^{1,2} · Dina V. Korchagina¹ · Dmitry S. Baev^{1,2} · Pavel M. Vassiliev³ · Konstantin P. Volcho^{1,2} · Nariman F. Salakhutdinov^{1,2}

Received: 4 February 2019 / Revised: 22 April 2019 / Accepted: 23 April 2019 / Published online: 22 May 2019
© The Author(s), under exclusive licence to the Japan Antibiotics Research Association 2019

Abstract

A number of substituted benzopentathiepin-6-amines and their analogues without a polysulfur ring were synthesized and evaluated in vitro for antimicrobial activity against a panel of reference bacterial and fungal strains. Trifluoroacetamide **14** demonstrated high antibacterial activity against *Staphylococcus aureus* (MRSA strain) with a MIC of 4 µg/mL, which was four-fold higher than the activity of a reference drug amoxicillin. This compound was also most active against the *Candida albicans* fungus (MIC of 1 µg ml⁻¹), whereas amide **17** containing a morpholine substituent was most active against the *Cryptococcus neoformans* fungus (MIC of 2 µg ml⁻¹). These compounds have no hemolytic activity and are low cytotoxic. Replacement of the pentathiepine ring with 1,3-dithiolan-2-one or 1,3-dithiolane moieties leads to loss of antimicrobial activity. Based on the QSAR analysis and molecular docking data, bacterial DNA ligase might be one of the targets for the antibacterial activity of substituted benzopentathiepin-6-amines against *S. aureus*.

Introduction

Bacterial resistance to known antibacterial agents is a serious problem in treatment of bacterial infections [1]. According to the World Health Organization (WHO), resistance to antibiotics is reaching dangerously high levels, threatening the ability to treat common infectious diseases [2]. Currently, most agents under development are modifications of existing antibiotics, whereas a search for antibiotics of new structural types and mechanisms of action is necessary to overcome the resistance [3]. A key role in the development of existing antibiotics and in the search for new antibiotics is played by compounds isolated from natural sources [4, 5].

An interesting type of natural compounds with pronounced antimicrobial activity is benzopentathiepin-6-amines isolated from marine invertebrates [6, 7]. For example, lissoclinotoxin A (**1**) (Fig. 1) isolated from the tunicate *Lissoclinum perforatum* [8] exhibited antifungal activity against *Candida albicans* (MIC of 40 µg ml⁻¹) and antibacterial activity against Gram-positive and Gram-negative bacteria (MIC of 0.1–0.6 µg ml⁻¹) [8, 9]. A methylated analogue of compound **1**, varacin **2**, was isolated from the ascidian *Lissoclinum vareau* [10] and *Polycitor sp* [11], and also demonstrated antifungal (against *C. albicans*) and antibacterial (against *Bacillus subtilis*) activities with inhibition zones of 20 mm at 0.1 µg/disk [11]. Synthetic varacin acetate **3** was significantly less active, with effective concentrations being 10 µg/disk for *C. albicans* and 1 µg/disk for *B. subtilis* [11]. Benzopentathiepine **4** containing an additional thiomethyl group, which was found in the ascidian *Lissoclinum japonicum*, exhibited antibacterial activity at relatively high doses (20–50 µg/disk) [12]. A serious obstacle to the practical use of these compounds is their low content in natural sources and their poor availability through synthesis [13] in combination with high cytotoxicity, which stimulates the search for their active, fully synthetic analogues [6]. For example, antifungal activity of synthetic benzopentathiepin-6-amines **5–9** against agricultural infections *Venturia inaequalis* (apple scab), *Magnaporthe grisea* (rice blast fungus), powdery mildew, and *Puccinia rust* fungus (wheat leaf rust) was demonstrated [14].

Supplementary information The online version of this article (<https://doi.org/10.1038/s41429-019-0191-y>) contains supplementary material, which is available to authorized users.

✉ Konstantin P. Volcho
volcho@nioch.nsc.ru

- ¹ Novosibirsk Institute of Organic Chemistry, Lavrentjev av. 9, Novosibirsk 630090, Russia
- ² Novosibirsk State University, Pirogova st. 1, Novosibirsk 630090, Russia
- ³ Volgograd State Medical University, Pavshikh Bortsov Sq. 1, Volgograd 400131, Russia

Fig. 1 Natural and synthetic benzopentathiepins with antimicrobial activity

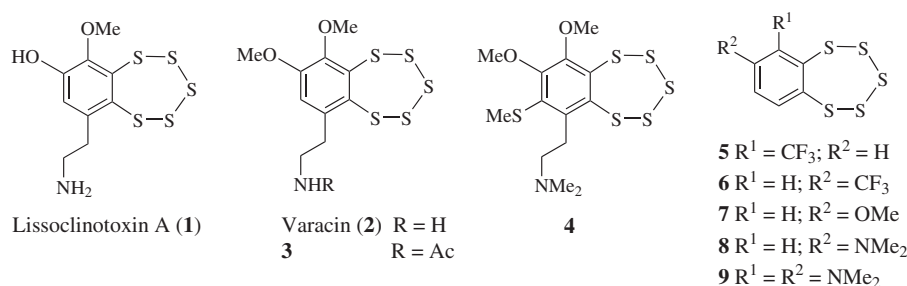
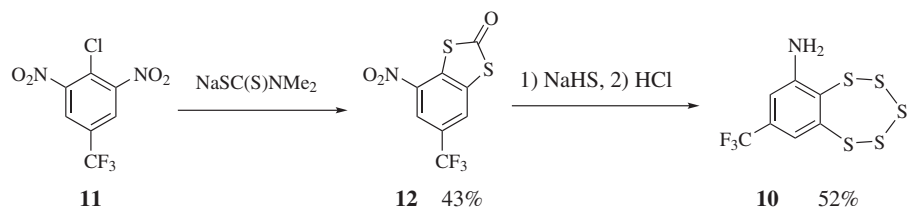


Fig. 2 Synthesis of compound **10**



Previously, we found a simple and effective method for synthesis of aminobenzopentathiepine **10** from 1-chloro-4-(trifluoromethyl)benzene **11**, with benzodithiol-2-one **12** being a key intermediate (Fig. 2) [15, 16]. Compound **10** and its hydrochloride, known as TC-2153, exhibited in vivo antidepressant properties and anti-Alzheimer activity [17–19], but antimicrobial activity of compound **10** or its derivatives was not studied previously. However, given moderate cytotoxicity [20, 21] and low acute toxicity [15] as well as good antimicrobial activity of benzopentathiepins **1–9**, investigation of antimicrobial properties of **10** and its derivatives seems to be promising. This was the aim of this study.

Results and discussion

Aminobenzopentathiepine **10** and its amides **13–17** were synthesized according to previously published methods (Fig. 3) [15, 20, 22]. Compounds **18** and **19**, analogues of trifluoroacetamide **14** without a pentathiepine ring, were produced from amines **20** and **21**.

Compound **20** was synthesized by reduction of a nitro group in **12** according to the method [19]. Two approaches were used for synthesis of amine **21**. When treated with bases, the pentathiepine ring is destroyed with loss of some sulfur atoms and formation of reactive dithiols [6]. The latter are easily alkylated (e.g., with alkyl dihalides $Hal(CH_2)_nHal$) to form new sulfur-containing heterocycles. Indeed, keeping amine **10** solution in CH_2Cl_2 in the presence of Et_3N at room temperature for 10 days led to the formation of compound **21**. The conversion of amine **10** under these conditions was 70%, and the yield of compound **21** (in calculation on the reacted amine **10**) was 51%.

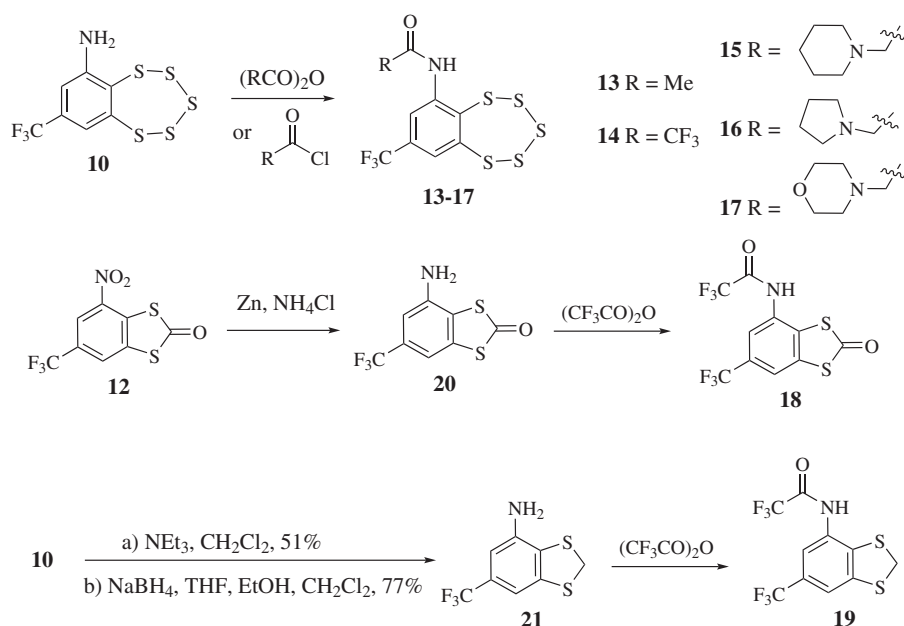
Another well-known reagent for synthesis of dithiols from pentathiepins is $NaBH_4$ [6]. If an electrophilic reagent (e.g., alkylene dihalide) is present in the reaction mixture, disulfur heterocycles are produced. We reduced the pentathiepine ring in compound **10** using $NaBH_4$, followed by addition of CH_2Cl_2 to the reaction mixture and keeping the mixture at room temperature for 5 days. In this case, complete conversion of amine **10** occurred, and the yield of compound **21** was 77%.

Antimicrobial activity of compounds **10**, **13–19** was studied by The Community for Antimicrobial Drug Discovery (CO-ADD) [23]. Compounds were tested against Gram-negative (*Escherichia coli*; *Klebsiella pneumoniae*, multiple drug resistance (MDR) strain; *Acinetobacter baumannii*; *Pseudomonas aeruginosa*) and Gram-positive (*Staphylococcus aureus*, methicillin-resistant (MRSA) strain) bacteria as well as against *C. albicans* and *Cryptococcus neoformans* fungi.

A. baumannii, *P. aeruginosa*, and Enterobacteriaceae, including *K. pneumoniae* and *E. coli*, can cause severe and often deadly infections, such as bloodstream infections and pneumonia [24]. MRSA strains also cause difficult-to-treat diseases in humans, such as sepsis and pneumonia, and are among the most dangerous nosocomial pathogens. The development of antibiotics for control of these bacteria is considered by the World Health Organization (WHO) as a high priority [24].

C. albicans and *C. neoformans* are important hospital pathogens, particularly dangerous in patients with immunodeficiency due to AIDS, cancer chemotherapy, or organ transplantation [25–27].

For the tested compounds, the minimum inhibitory concentration (MIC), the lowest concentration that inhibits visible growth of microorganisms and is usually reported as a 80% MIC value, was determined. As reference drugs, we

Fig. 3 Synthesis of compounds **13–21****Table 1** Antimicrobial activity of compounds

Compound	MIC ($\mu\text{g ml}^{-1}$) ^{a,b}			CC ₅₀ ^c ($\mu\text{g ml}^{-1}$)	Hc ₁₀ ^d ($\mu\text{g ml}^{-1}$)
	<i>S. aureus</i>	<i>C. albicans</i>	<i>C. neoformans</i>		
10	16	8	16	>32	>32
13 (R = CH ₃)	4	2	4	5.44	>32
14 (R = CF ₃)	4	1	8	>32	>32
15 (R = CH ₂ Pyr)	16	8	8	>32	>32
16 (R = CH ₂ Pyrr)	16	8	8	>32	26.86
17 (R = CH ₂ Morph)	>32	>32	2	>32	>32
18	>32	>32	>32	>32	>32
19	>32	32	32	>32	>32
Vancomycin	1	–	–	–	–
Amoxicillin	16	–	–	–	–
Fluconazole	–	0.125	8	–	–

^aMIC was determined as the lowest concentration at which the growth was fully inhibited, defined by an inhibition $\geq 80\%$

^b*S. aureus*—*Staphylococcus aureus* (ATCC 43300 MRSA); *C. albicans*—*Candida albicans* (ATCC 90028 CLSI reference); *C. neoformans*—*Cryptococcus neoformans* (ATCC 208821 H99 - Type strain)

^cConcentration at 50% cytotoxicity

^dConcentration at 10% haemolytic activity

used vancomycin and amoxicillin for antibacterial activity and fluconazole for antifungal activity.

All compounds containing the pentathiepine ring (**10** and **13–17**), as well as their analogues **18** and **19**, had no activity against Gram-negative bacteria (MIC > 32 $\mu\text{g ml}^{-1}$).

The results of testing against Gram-positive *S. aureus* MRSA and fungal pathogens are presented in Table 1.

The obtained data demonstrate that the parent aminobenzopentathiepine **10** has moderate antibacterial activity

against *S. aureus*, with a MIC of 16 $\mu\text{g ml}^{-1}$. Similar results were obtained for amides **15** and **16** and the reference drug amoxicillin, while amide **17** containing an additional heteroatom in the lateral substituent was completely inactive. At the same time, the use of acetamide **13** and trifluoroacetamide **14** resulted in a fourfold increase in the activity, with the MIC reaching 4 $\mu\text{g ml}^{-1}$. The activity of compounds **13** and **14** is superior to that of the reference drug amoxicillin and only slightly lower than that of

vancomycin. The lack of antibacterial activity in compounds **18** and **19**, analogues of compound **14**, which do not contain a polysulfur ring, indicates that the pentathiepine ring is essential for the activity.

Compounds **13** and **14** were also most active against *C. albicans*, with a MIC of 1 and 2 $\mu\text{g ml}^{-1}$, respectively (Table 1). In this case, a significant antifungal effect was exhibited by parent compound **10** as well as by amides **15** and **16**. Compounds **17** and **18** were not active, whereas benzo [1, 3]dithiole **19** exhibited moderate activity, with a MIC of 32 $\mu\text{g ml}^{-1}$.

Compound **17** was most active against *C. neoformans*, but had no activity in other tests; acetamide **13** was the second active compound (Table 1). It should be noted that both compounds were more active than the reference drug fluconazole. The activity of compounds **14–16** was comparable to that of fluconazole, while compounds **10** and **19** were somewhat less active.

An extremely important feature of antimicrobial agents is their toxicity. Therefore, all compounds were tested for cytotoxicity and hemolytic activity, which were also examined by CO-ADD.

Cytotoxicity was determined on HEK293 cells. Of all the tested compounds, only acetamide **13** exhibited high cytotoxicity, while CC_{50} (50% cytotoxic concentration) of other compounds exceeded 32 $\mu\text{g ml}^{-1}$ (Table 1). All tested compounds had no hemolytic activity against red blood cells at a dose of 32 $\mu\text{g ml}^{-1}$, except compound **16** with a HC_{10} (10% hemolytic concentration) of 27 $\mu\text{g ml}^{-1}$.

Therefore, given the combination of high activity and low cytotoxicity, the most promising compounds for further studies are trifluoroacetamide **14** for control of *S. aureus* and *C. albicans* and compound **17** as an antimycotic agent against *C. neoformans*.

At present, there is no literature data on potential targets associated with the antimicrobial properties of benzopentathiepines. While the antimicrobial properties of highly cytotoxic compounds, such as varacin **2**, may be related to the ability of some pentathiepines to damage cellular DNA [28], other targets should be identified for non-toxic compounds.

To identify potential biotargets associated with the antibacterial activity of pentathiepines, we performed in silico prediction of their inhibitory activity levels against 43 different target proteins of *S. aureus* using the Microcosm BioS v18.1.9 system. The QSAR database of Microcosm BioS contains verified, structured, and processed information on the chemical structure and activity of 625,888 known compounds (derived from ChEMBL [29], BindingDB [30], and PubChem [31]) that have been screened by the world scientific community for 11,509 target biological activities (as of 04.11.2017). The QSAR database was formed using the Microcosm software [32]. The range of

values for each activity type was divided into deciles. Each decile interval was assigned a fixed activity index value, from $\text{Ind}_{\text{Act}} = -5$ (inactive) to $\text{Ind}_{\text{Act}} = +5$ (highly active).

The spectrum of target activity levels for a new compound was predicted using the 2D structural similarity method. The Microcosm BioS program finds in the QSAR database a specified number of tested compounds (20 in this study) that are structurally most similar to the predicted molecule. All tested activities are listed for each found analogue, with an activity index value being indicated for each activity.

To assess proteins of *S. aureus* as relevant biotargets for the antimicrobial activity of benzopentathiepines **10** and **13–17**, the total number of the nearest tested analogues for the five compounds (in comparison with QSAR database filling, ID is an identifier of protein in UniProtKB [33]) and the mean activity index value were determined for each target (Table 2).

According to the calculation results, the most promising biotargets related to the antimicrobial activity of pentathiepines are DNA ligase and tRNAsynthetase (Phenylalanine-tRNA ligase). The last enzyme consists of two protein subunits: P68849 (Phenylalanine-tRNA ligase alpha subunit) and Q9AGR3 (Phenylalanine-tRNA ligase beta subunit) which are expressed by different genes. According to the prediction in Microcosm BioS, it is impossible to define exactly which of these two proteins could be affected by new substances. In addition, there are no experimental X-ray models of 3D structures for *S. aureus* for these proteins in PDB. Therefore, this hybrid target was excluded from further consideration.

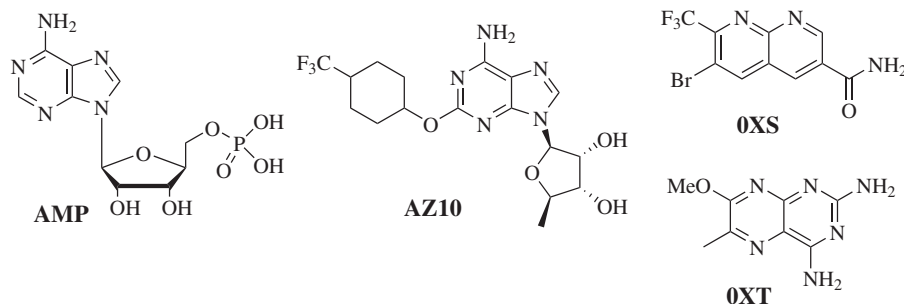
Among 69 compounds tested for DNA ligase inhibition, 14 structural analogues of compounds **10** and **13–17** were found; their mean activity index was $\text{Ind}_{\text{Act}} = 0.9$, which was higher than the mean activity ($\text{Ind}_{\text{Act}} = 0$ corresponds to the median). The other analyzed biotargets were less promising because their mean activity indices were less than zero, from $\text{Ind}_{\text{Act}} = -1.0$ (less than the mean level) to $\text{Ind}_{\text{Act}} = -4.0$ (very low activity).

Bacterial DNA ligase is an NAD^{+} -dependent enzyme involved in DNA replication [34]. Bacterial DNA ligase is essential for viability of both Gram-positive and Gram-negative bacteria and is phylogenetically distinct from its human, ATP-dependent, counterpart [35]. These data indicate that bacterial DNA ligase is a promising target for new generation antibacterial drugs.

To simulate a potential mechanism of DNA ligase inhibition, molecular docking of compounds **10** and **13–19** into the adenosine monophosphate (AMP) binding site was done. Molecular modeling was performed with the Schrodinger Maestro visualization program using applications from the Schrodinger Small Molecule Drug Discovery Suite 2017–1 package [36]. Three-dimensional structures of the

Table 2 In silico prediction of an inhibitory activity for various protein-targets of *Staphylococcus aureus*

Target	ID ^a	Gene	$N_{MC-BioS}^b$	$K_{Nearest}^c$	Ind_{Act}^d
Dihydrofolatereductase (DHFR)	G8GLL0	<i>dhfr</i>	109	10	-2.3
DNA gyrase subunit B	P0A0K8	<i>gyrB</i>	139	5	-1.2
DNA ligase	Q9AIU7	<i>ligA</i>	69	14	0.9
Enoyl-ACP reductase (FabI)	G3G998	<i>fabI</i>	178	5	-1.0
MurE — UDP-N-acetylmuramoyl-L-alanyl-D-glutamate-L-lysine ligase (strain Mu50/ATCC 700699)	P65479	<i>murE</i>	12	3	-1.3
Peptide deformylase (strain Mu50/ATCC 700699)	P68825	<i>def</i>	46	36	-2.4
Pyruvate kinase (strain MRSA252)	Q6GG09	<i>Pyk</i>	67	2	-4.0
Sortase A (SrtA) — Class A sortase SrtA	Q9S446	<i>srtA</i>	187	8	-3.0
tRNA synthetase (Phenylalanine-tRNA ligase alpha subunit & Phenylalanine-tRNA ligase beta subunit)	P68849 & Q9AGR3	<i>pheS</i> & <i>pheT</i>	45	23	0.7

^aIdentifier of protein in UniProtKB [33]^bNumber of tested substances for this activity in QSAR-base of Microcosm BioS v18.1.9^cNumber of most structurally similar compounds with this activity among the 20 nearest neighbors, for benzopentathiepins **10**, **13–17**^dAverage index of activity level of the most structurally similar compounds, for benzopentathiepins **10**, **13–17****Fig. 4** Structures of AMP and known bacterial DNA ligase inhibitors

derivatives were obtained empirically in the *LigPrep* application using the OPLS3 force field [37]. All possible tautomeric forms of compounds, as well as various states of molecules in the pH range of 7.0 ± 2.0 were taken into account. A XRD model of the interaction between *E. coli* DNA ligase and a new compound from a series of 2-amino-[1, 8]-naphthyridine-3-carboxamides with PDB ID 4GLX (1.9 Å resolution) was chosen [38]. To model a possible mechanism of inhibition of selected target molecular docking of new compounds was performed at the binding site of AMP using Glide application [39]. The search area for docking (docking grid) was selected automatically, based on the size and physico-chemical properties of inhibitors from chosen XRD model. The extra precision (XP) algorithm of docking was applied. Docking was done in comparison with previously studied inhibitors **OXS** and **OXT** [38] as well as an AstraZeneca's patented adenosine derivative **AZ10** (Fig. 4) [40]. The three-dimensional structures of inhibitors were obtained in the PubChem database and prepared in the *LigPrep* application.

The minimum binding energy values were found using the molecular docking procedure described above (Table 3).

As expected, adenosine monophosphate, being a natural ligase ligand, demonstrates the best estimated binding

energy. In the used model, the adenosine derivative **AZ10** is a synthetic ligand with the highest affinity. Interestingly, compound **16** exhibits an estimated binding energy very close to that of **AZ10** and significantly higher than that of the reference ligand **OXS** of the selected model. In general, all pentathiepine amides are characterized by estimated binding energies comparable to the energy obtained for **OXT**. The lowest binding energies are predicted for lissoclinotoxin A (**1**) (Fig. 1) and amine **10**.

Figure 5 shows features of non-covalent interactions of pentathiepins **16** and **17** in comparison with **AZ10** and **OXS** inhibitors.

Known adenosine inhibitors form hydrogen bonds between heterocyclic and amino group nitrogens and amino acid residues Glu113, Leu114, Lys115, and Lys290 [38]. Stacking interactions between heterocyclic π -systems of inhibitors and the Tyr225 residue have an important coordinating function. The main difference in binding of new pentathiepins to the AMP binding site of DNA ligase is the absence of hydrogen bonds with 113–115 amino acid residues. However, there are possible stable interactions with the Tyr225 residue. Furthermore, compound **16** stacks with the residue similarly to the studied inhibitors and AMP, whereas compounds **15** and **17** form hydrogen bonds

with a hydroxyl group of this amino acid residue. The Lys290 residue marked by the authors of a model [38] forms hydrogen bonds with compounds **15** and **16**. It is also

Table 3 The values of the minimum binding energy of compounds with DNA ligase active site

Ligand	Binding energy, kcal/mol ^a	Ligand	Binding energy, kcal/mol ^a
AMP	-11.003	0XT	-7.292
AZ10	-10.484	18	-7.285
16	-10.271	14	-7.013
0XS	-8.561	1	-6.515
17	-8.254	19	-6.171
15	-7.498	10	-6.156

^aIt is not a true binding energy and should be considered as an estimated value (docking score)

worth noting hydrogen bonds that may be formed by Leu80. The hydrogen bonds are formed both with AMP and with new tested compounds. In the case of **0XS**, this residue is involved in the formation of a halogen bond with the inhibitor bromine atom. A feature of new compounds is active involvement of sulfur atoms of pentathiepine rings both in the formation of hydrogen bonds (with Arg171 for compounds **15** and **16**) and in interactions with π -systems (all analyzed compounds).

In addition to the main AMP binding site, bacterial DNA ligase may have additional binding sites [41]. To examine possible binding of pentathiepine derivatives to alternative binding sites on the DNA ligase surface, an X-ray structural model (PDB ID 4GLX) was mapped using the CASTp 3.0 computational algorithm [42]. Then, sites were selected based on the criteria of at least one entrance and an internal volume exceeding 10 \AA^3 . Molecular docking into the

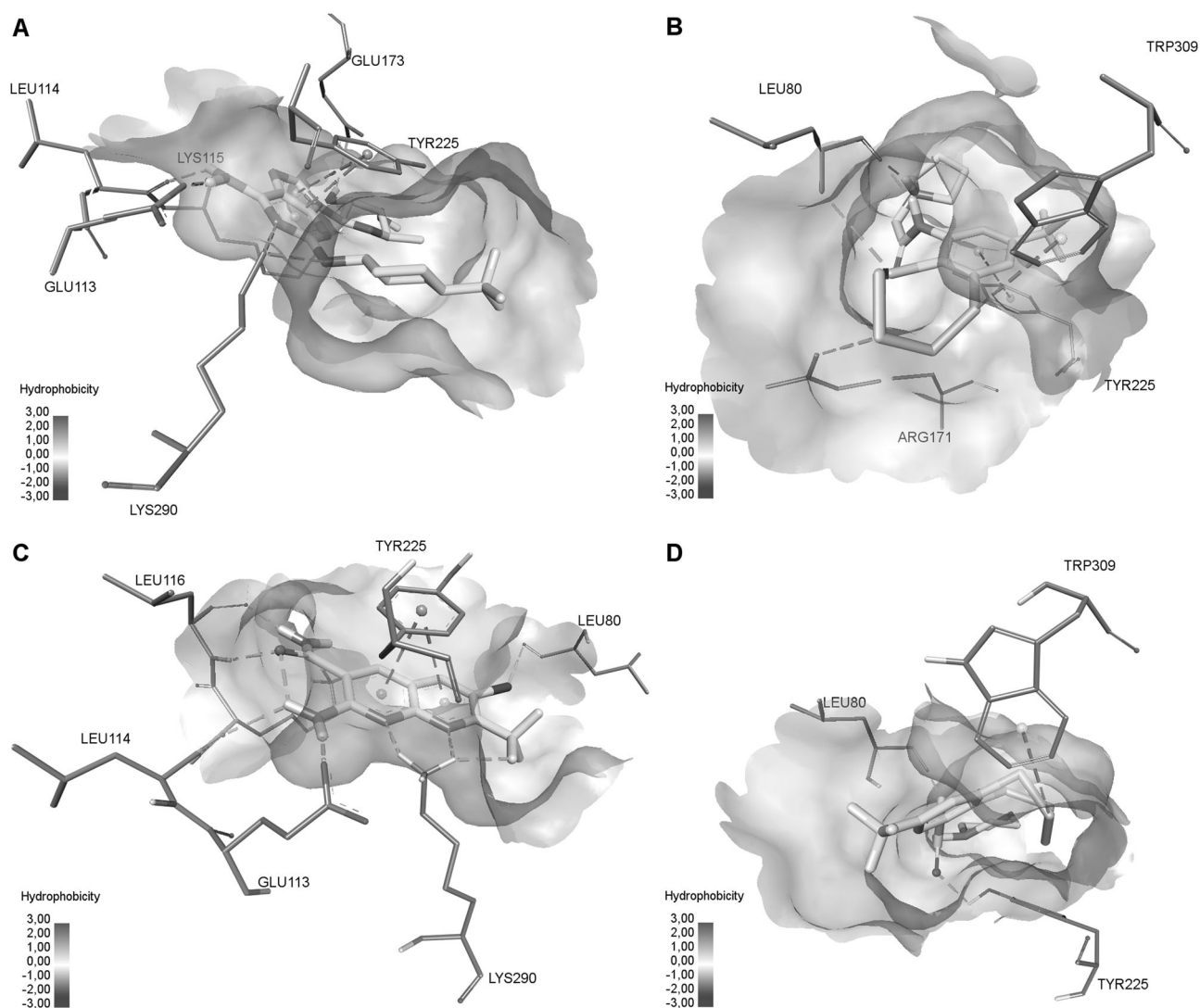


Fig. 5 Non-covalent interactions of compounds in the AMP binding site of bacterial DNA ligase: **A** – **AZ10**; **B** – **16**; **C** – **0XS**; **D** – **17**. The binding site surface is colored according to the degree of

hydrophobicity. Non-covalent interactions are denoted by dashed lines: hydrogen bonds (green); π -system interactions (violet); interactions of sulfur atoms (yellow); halogen bonds (blue)

selected sites was done. The estimated binding energy (docking score) of all simulated compounds was found to be less than 5.7 kcal/mol (Tables S1–S5, Supporting information), which excludes involvement of these sites in the action mechanism of studied compounds.

Therefore, bacterial DNA ligase is a potential target for new pentathiepine derivatives. At the same time, the lack of a clear correlation between the calculated data and antibacterial activity suggests that the studied compounds may have other targets.

Conclusion

In conclusion, we synthesized a number of substituted benzopentathiepine-6-amines and their analogues lacking a polysulfur ring. Parent amine **10** and amides **13–16** derived from it were highly active against Gram-positive bacteria (*S. aureus*, MRSA strain). The most active compounds were acetamide **13** and trifluoroacetamide **14**, with a MIC of 4 $\mu\text{g ml}^{-1}$, which was four-fold higher than activity of the reference drug amoxicillin. The same compounds were most active against the *C. albicans* fungus (MIC of 1 to 2 $\mu\text{g ml}^{-1}$). All amides comprising the benzopentathiepine backbone were active against the *C. neoformans* fungus; of these, the most effective compound was amide **17** was (MIC of 2 $\mu\text{g ml}^{-1}$) containing a morpholine substituent and being four-fold more active than the reference drug fluconazole. Replacement of the pentathiepine ring with 1,3-dithiolan-2-one or 1,3-dithiolane moieties led to disappearance of the antimicrobial activity. All studied compounds had no hemolytic activity and, except acetamide **13**, were low cytotoxic. Given the combination of high activity and low cytotoxicity, the most promising compounds for further research are trifluoroacetamide **14** as an agent to control *S. aureus* and *C. albicans* and compound **17** as an antimycotic agent against *C. neoformans*.

On the basis of the QSAR analysis and molecular docking data, bacterial DNA ligase might be one of the targets for antibacterial activity of new benzopentathiepines against *S. aureus*.

Experimental

General

Reagents and solvents were purchased from commercial suppliers and used as received. 8-(Trifluoromethyl)benzo[*f*][1–5]pentathiepin-6-amine **10** and amides **13**, **14** were synthesized in accordance with [15]. Compounds **15–17** were synthesized as described in [20].

GC-MS: *Agilent 7890A* gas chromatograph equipped with a quadrupole mass spectrometer *Agilent 5975C* as a detector; quartz column HP-5MS (copolymer 5%–diphenyl–95%–dimethylsiloxane) of 30 m length, internal diameter 0.25 mm and stationary phase film thickness 0.25 μm . ^1H and ^{13}C NMR: *Bruker DRX-500* apparatus at 500.13 MHz (^1H) and 125.76 MHz (^{13}C), *J* in Hz; structure determinations by analyzing the ^1H NMR spectra, including ^1H – ^1H double resonance spectra, *J*-modulated ^{13}C NMR spectra (JMOD), ^{13}C NMR spectra using proton off-resonance saturation and at times ^{13}C – ^1H 2D heteronuclear correlation long-range spin-spin coupling constants (COLOC, $^{2,3}J(\text{C},\text{H}) = 10$ Hz). HR-MS: DFS Thermo Scientific spectrometer in a full scan mode (15–500 *m/z*, 70 eV electron impact ionization, direct sample administration).

6-(Trifluoromethyl)benzo[*d*][1,3]dithiol-4-amine (21)

(A) Et_3N (0.15 g, 1.5 mmol) was added with stirring to the solution of compound **10** (0.44 g, 1.38 mmol) in CH_2Cl_2 (7 ml). The mixture was stirred for 10 days at room temperature. Then water (8 ml) and CH_2Cl_2 (2 ml) were added to the reaction mixture. The products were extracted by CH_2Cl_2 , dried over Na_2SO_4 . The solvent was distilled off, and the residue was separated by column chromatography: silica gel (SiO_2 ; 60–200 μ ; *Macherey-Nagel*); hexane/benzene (1:1), CH_2Cl_2 . Amine **21** (0.118 g, yield 51%, calculated on consumed **10** (conversion 70%)).

(B) NaBH_4 (0.127 g, 3.36 mmol) was added with stirring to the solution of compound **10** (0.155 g, 0.49 mmol) in THF (5 ml) and EtOH (2 ml). The mixture was stirred for 30 min at room temperature, then CH_2Cl_2 (1 ml) was added. The mixture was stirred for 5 days at room temperature. Then water (4 ml) and CH_2Cl_2 (2 ml) were added to the reaction mixture. The products were extracted by CH_2Cl_2 , dried over Na_2SO_4 . The solvent was distilled off, and the residue was separated by column chromatography: silica gel (SiO_2 ; 60–200 μ ; *Macherey-Nagel*); hexane/benzene (1:1), CH_2Cl_2 . Amine **21** (0.089 g, yield 77%). HRMS: 235.9809 $[\text{M}-\text{H}]^+$; calcd. 235.9810 ($\text{C}_8\text{H}_5\text{NF}_3\text{S}_2$). ^1H NMR (500 MHz, CDCl_3) δ 3.82 (br s, NH_2), 4.34 (s, 2H-3), 6.60 (d q, H-7, $J_{7,5}$ 1.5 Hz, $J_{7,\text{F}}$ = 0.7 Hz), 6.89 (d q, H-5, $J_{5,7}$ 1.5 Hz, $J_{5,\text{F}}$ 0.7 Hz). ^{13}C NMR (125.8 MHz, CDCl_3) δ 141.12 (s, C-1), 126.10 (s, C-2), 36.42 (t, C-3), 140.27 (s, C-4), 109.39 (C-5, $^3J_{\text{C},\text{F}}$ 4.0 Hz), 129.36 (C-6, $^2J_{\text{C},\text{F}}$ 32.7 Hz), 109.10 (C-7, $^3J_{\text{C},\text{F}}$ 4.0 Hz), 123.74 (C-8, $^1J_{\text{C},\text{F}}$ 272.0 Hz).

2,2,2-Trifluoro-*N*-(2-oxo-6-(trifluoromethyl)benzo[*d*][1,3]dithiol-4-yl)acetamide (18)

$(\text{CF}_3\text{CO})_2\text{O}$ (0.1 ml, 0.72 mmol) was added with stirring to the solution of compound **20** (0.072 g, 0.29 mmol) in CH_2Cl_2 (0.5 ml). The mixture was stirred for 2 h at room

temperature. The solvent was distilled off to give 0.085 g (84%) 2,2,2-trifluoro-*N*-(2-oxo-6-(trifluoromethyl)benzo[*d*][1,3]dithiol-4-yl)acetamide **18**. M.p.: 187 °C. HRMS: 346.9499 [M]⁺; calcd. 346.9504 (C₁₀H₃O₂NS₂F₆). ¹H NMR (500 MHz, CDCl₃ + CD₃OD) δ 7.64 (br s, H-7), 7.68 (d q, H-5, *J*_{5,7} 1.7 Hz, *J*_{5,F} 0.7 Hz). ¹³C NMR (125.8 MHz, CDCl₃ + CD₃OD) δ 134.53 (s, C-1), 129.93 (s, C-2), 186.68 (s, C-3), 133.10 (s, C-4), 118.33 (C-5, ³*J*_{C,F} 3.8 Hz), 129.78 (C-6, ²*J*_{C,F} 34.2 Hz), 120.87 (C-7, ³*J*_{C,F} 3.8 Hz), 122.71 (C-8, ¹*J*_{C,F} 272.8 Hz), 155.72 (C-9, ²*J*_{C,F} 38.7 Hz), 115.46 (C-10, ¹*J*_{C,F} 287.9 Hz).

2,2,2-Trifluoro-*N*-(6-(trifluoromethyl)benzo[*d*][1,3]dithiol-4-yl)acetamide (**19**)

(CF₃CO)₂O (0.25 ml, 1.79 mmol) was added with stirring to the solution of compound **21** (0.170 g, 0.72 mmol) in CH₂Cl₂ (2 ml). The mixture was stirred for 2 h at room temperature. The solvent was distilled off to give 0.229 g (95%) 2,2,2-trifluoro-*N*-(6-(trifluoromethyl)benzo[*d*][1,3]dithiol-4-yl)acetamide **19**. M.p.: 136 °C. HRMS: 331.9631 [M-H]⁺; calcd. 331.9633 (C₁₀H₄O₁N₁F₆S₂). ¹H NMR (500 MHz, CDCl₃) δ 4.62 (s, 2H-3), 7.33 (br s, H-5), 7.62 (br s, NH), 7.87 (br s, H-7). ¹³C NMR (125.8 MHz, CDCl₃) δ 129.74 (s, C-1), 135.16 (s, C-2), 37.06 (t, C-3), 141.77 (s, C-4), 116.79 and 116.99 (C-5, C-7, ³*J*_{C,F} 3.9 Hz), 129.53 (C-6, ²*J*_{C,F} 33.5 Hz), 123.09 (C-8, ¹*J*_{C,F} 272.5 Hz), 154.86 (C-9, ²*J*_{C,F} 38.1 Hz), 115.31 (C-10, ¹*J*_{C,F} 288.7 Hz).

Biology

Antimicrobial screening was performed by CO-ADD (The Community for Antimicrobial Drug Discovery), Australia [23].

Antibacterial assay

Procedure

All bacteria (*S. aureus* (Strain ATCC 43300, MRSA), *E. coli* (Strain ATCC 25922, FDA control strain), *K. pneumoniae* (Strain ATCC 700603, MDR), *A. baumannii* (Strain ATCC 19606, Type strain), *P. aeruginosa* (Strain ATCC 27853, Quality control strain) were cultured in Cation-adjusted Mueller Hinton broth (CAMHB) at 37 °C overnight. A sample of each culture was then diluted 40-fold in fresh broth and incubated at 37 °C for 1.5–3 h. The resultant mid-log phase cultures were diluted (CFU/ml measured by OD₆₀₀), then added to each well of the compound containing plates, giving a cell density of 5 × 10⁵ CFU/ml and a total volume of 50 μl. All the plates were covered and incubated at 37 °C for 18 h without shaking.

Analysis

Inhibition of bacterial growth was determined measuring absorbance at 600 nm (OD₆₀₀), using a Tecan M1000 Pro monochromator plate reader. The percentage of growth inhibition was calculated for each well, using the negative control (media only) and positive control (bacteria without inhibitors) on the same plate as references.

The percentage of growth inhibition was calculated for each well, using the negative control (media only) and positive control (bacteria without inhibitors) on the same plate. The MIC was determined as the lowest concentration at which the growth was fully inhibited, defined by an inhibition ≥80%.

The results are listed in the Table 1.

Antifungal assay

Procedure

Fungi strains (*C. albicans* (Strain ATCC 90028, CLSI reference, *C. albicans*) and *C. neoformans* (Strain ATCC 208821, H99 Type strain, *C. neoformans*)), were cultured for 3 days on Yeast Extract-Peptone Dextrose (YPD) agar at 30 °C. A yeast suspension of 1 × 10⁶ to 5 × 10⁶ CFU/ml (as determined by OD₅₃₀) was prepared from five colonies. The suspension was subsequently diluted and added to each well of the compound-containing plates giving a final cell density of fungi suspension of 2.5 × 10³ CFU/ml and a total volume of 50 μl. All plates were covered and incubated at 35 °C for 36 h without shaking.

Analysis

Growth inhibition of *C. albicans* was determined measuring absorbance at 630 nm (OD₆₃₀), while the growth inhibition of *C. neoformans* was determined measuring the difference in absorbance between 600 and 570 nm (OD_{600–570}), after the addition of resazurin (0.001% final concentration) and incubation at 35 °C for 2 h. The absorbance was measured using a Biotek Multiflo Synergy HTX plate reader.

In both cases, the percentage of growth inhibition was calculated for each well, using the negative control (media only) and positive control (fungi without inhibitors) on the same plate. The MIC was determined as the lowest concentration at which the growth was fully inhibited, defined by an inhibition ≥80% for *C. albicans* and an inhibition ≥70% for *C. neoformans*. Due to a higher variance in growth and inhibition, a lower threshold was applied to the data for *C. neoformans*.

The results are listed in the Table 1.

Cytotoxicity assay

Procedure

HEK293 cells were counted manually in a Neubauer haemocytometer and then plated in the 384-well plates containing the compounds to give a density of 6000 cells/well in a final volume of 50 μ l. DMEM supplemented with 10% FBS was used as growth media and the cells were incubated together with the compounds for 20 h at 37 °C in 5% CO₂.

Analysis

Cytotoxicity (or cell viability) was measured by fluorescence, ex: 560/10 nm, em: 590/10 nm (F_{560/590}), after addition of 5 μ l of 25 μ g ml⁻¹ Resazurin (2.3 μ g ml⁻¹ final concentration) and after incubation for further 3 h at 37 °C in 5% CO₂. The fluorescence intensity was measured using a Tecan M1000 Pro monochromator plate reader, using automatic gain calculation

CC₅₀ (concentration at 50% cytotoxicity) were calculated by curve fitting the inhibition values vs. log(concentration) using sigmoidal dose-response function, with variable fitting values for bottom, top and slope.

Acknowledgements The antimicrobial screening performed by CO-ADD (The Community for Antimicrobial Drug Discovery) was funded by the Wellcome Trust (UK) and The University of Queensland (Australia). We would like to acknowledge the Multi-Access Chemical Research Center SB RAS for spectral and analytical measurements. This work was supported by SB RAS integration project (N 0302–2018–0010).

Compliance with ethical standards

Conflict of interest The authors declare that they have no conflict of interest.

Publisher's note: Springer Nature remains neutral with regard to jurisdictional claims in published maps and institutional affiliations.

References

- Brown ED, Wright GD. Antibacterial drug discovery in the resistance era. *Nature*. 2016;529:336–43.
- WHO. Antibiotic resistance. 2017. <http://www.who.int/mediacentre/factsheets/antibiotic-resistance/en/>.
- World Health Organization. Antibacterial agents in clinical development. 2017. WHO/EMP/IAU/2017.11.
- Aminov R. History of antimicrobial drug discovery: major classes and health impact. *Biochem Pharm*. 2017;133:4–19.
- Rossiter SE, Fletcher MH, Wuest WM. Natural products as platforms to overcome antibiotic resistance. *Chem Rev*. 2017;117:12415–74.
- Konstantinova LS, Amelichev SA, Rakitin OA. 1,2,3,4,5-Pentathiepinines and 1,2,3,4,5-pentathiepanes. *Russ Chem Rev*. 2007;76:195–211.
- Davison EK, Sperry J. Natural products with heteroatom-rich ring systems. *J Nat Prod*. 2017;80:3060–79.
- Litaudon M, Trigalo F, Martin M, Frappier F, Guyot M. Lissoclinotoxins: antibiotic polysulfur derivatives from the tunicate *Lissoclinum perforatum*. Revised structure of lissoclinotoxin A. *Tetrahedron*. 1994;50:5323–34.
- Litaudon M, Guyot M. Lissoclinotoxin A, an antibiotic 1,2,3-trithiane derivative from the tunicate *Lissoclinum perforatum*. *Tetrahedron Lett*. 1991;32:911–4.
- Davidson BS, Molinski TF, Barrows LR, Ireland CM. Varacin: a novel benzopentathiepin from *Lissoclinum vareau* that is cytotoxic toward a human colon tumor. *J Am Chem Soc*. 1991;113:4709–10.
- Makarievna TN, Stonik VA, Dmitrenok AS, Grebnev BB, Isakov VV, Rebachyk NM, et al. Varacin and three new marine antimicrobial polysulfides from the far-eastern ascidian *Polycitor* sp. *J Nat Prod*. 1995;58:254–8.
- Liu H, Fujiwara T, Nishikawa T, Mishima Y, Nagai H, Shida T, et al. Lissoclibadins 1–3, three new polysulfur alkaloids, from the ascidian *Lissoclinum cf. badium*. *Tetrahedron*. 2005;61:8611–5.
- Ford PW, Davidson BS. Synthesis of varacin, a cytotoxic naturally occurring benzopentathiepin isolated from a marine ascidian. *J Org Chem*. 1993;58:4522–3.
- Chenard BL. Substituted benzopentathiepins, process therefor and intermediates. Patent WO1984004921, 1984.
- Khomenko TM, Tolstikova TG, Bolkunov AV, Dolgikh MP, Pavlova AV, Korchagina DV, et al. 8-(Trifluoromethyl)-1,2,3,4,5-benzopentathiepin-6-amine: novel aminobenzopentathiepin having in vivo anticonvulsant and anxiolytic activities. *Lett Drug Des Discov*. 2009;6:464–7.
- Khomenko TM, Korchagina DV, Komarova NI, Volcho KP, Salakhutdinov NF. Synthesis of 6-Amino-benzopentathiepinines by reactions of 4-nitro-benzylthiol-2-ones with NaHS. *Lett Org Chem*. 2011;8:193–7.
- Kulikov AV, Tikhonova MA, Kulikova EA, Volcho KP, Khomenko TM, Salakhutdinov NF, et al. A new synthetic varacin analogue, 8-(trifluoromethyl)-1,2,3,4,5-benzopentathiepin-6-amine hydrochloride (TC-2153), decreased hereditary catalepsy and increased the BDNF gene expression in the hippocampus in mice. *Psychopharmacology*. 2012;221:469–78.
- Kulikova EA, Volcho KP, Salakhutdinov NF, Kulikov AV. Benzopentathiepin derivative, 8-(trifluoromethyl)-1,2,3,4,5-benzopentathiepin-6-amine hydrochloride (TC-2153), as a promising antidepressant of new generation. *Lett Drug Des Discov*. 2017;14:974–84.
- Xu J, Chatterjee M, Baguley TD, Brouillette J, Kurup P, Ghosh D, et al. Inhibitor of the tyrosine phosphatase STEP reverses cognitive deficits in a mouse model of Alzheimer's disease. *PLoS Biol*. 2014;12:e1001923.
- Zakharenko A, Khomenko T, Zhukova S, Koval O, Zakharova O, Anarbaev R, et al. Synthesis and biological evaluation of novel tyrosyl-DNA phosphodiesterase I inhibitors with a benzopentathiepin moiety. *Bioorg Med Chem*. 2015;23:2044–52.
- Kuzmich AS, Khomenko TM, Fedorov SN, Makarievna TN, Shubina LK, Komarova NI, et al. Cytotoxic and cancer preventive activity of benzotrithioles and benzotrithiole oxides, synthetic analogues of varacins. *Med Chem Res*. 2017;26:397–404.
- Baguley TD, Nairn AC, Lombroso PJ, Ellman JA. Synthesis of benzopentathiepin analogs and their evaluation as inhibitors of the phosphatase STEP. *Bioorg Med Chem Lett*. 2015;25:1044–6.
- Blaskovich MA, Zuegg J, Elliott AG, Cooper MA. Helping chemists discover new antibiotics. *ACS Infect Dis*. 2015;1:285–7.
- WHO. Global priority list of antibiotic-resistant bacteria to guide research, discovery, and development of new antibiotics. 2017. <http://www.who.int/mediacentre/news/releases/2017/bacteria-antibiotics-needed/en/>.

25. Pfaller MA, Diekema DJ. Epidemiology of invasive candidiasis: a persistent public health problem. *Clin Microbiol Rev.* 2007;20:133–63. <https://doi.org/10.1128/CMR.00029-06>.
26. Husain S, Wagener MM, Singh N. *Cryptococcus neoformans* infection in organ transplant recipients: variables influencing clinical characteristics and outcome. *Emerg Infect Dis.* 2001;7:375–81.
27. Mitchell TG, Perfect JR. Cryptococcosis in the era of AIDS—100 years after the discovery of *Cryptococcus neoformans*. *Clin Microbiol Rev.* 1995;8:515–48.
28. Lee SH. Disulfide and multisulfide antitumor agents and their modes of action. *Arch Pharm Res.* 2009;32:299–315.
29. ChEMBL: ChEMBL is a manually curated database of bioactive molecules with drug-like properties. 'Official site of the European Bioinformatics Institute of the European Molecular Biology Laboratory (EMBL-EBI). Hinxton, Cambridgeshire, UK. 2017. <https://www.ebi.ac.uk/chembl/>.
30. BindingDB: The Binding Database. BindingDB is a public web-accessible database of measured binding affinities. Official site of Skaggs School of Pharmacy and Pharmaceutical Sciences at the University of California. San Diego, La Jolla, CA, USA. 2017. <https://www.bindingdb.org/>.
31. PubChem. PubChem is world's largest collection of freely accessible chemical information. Official site of National Library of Medicine of National Center for Biotechnology Information of National Institutes of Health. Rockville Pike, Bethesda, MD, USA. 2017. <https://pubchem.ncbi.nlm.nih.gov>.
32. Vassiliev PM, Spasov AA, Kosolapov VA, Kucheryavenko AF, Gurova NA, Anisimova VA. Consensus Drug Design Using IT Microcosm. In: Application of Computational Techniques in Pharmacy and Medicine; Eds. L. Gorb, V. Kuz'min, E. Muratov. Series: Challenges and Advances in Computational Chemistry and Physics, vol. 17; Ed. J. Leszczynski. Dordrecht (Netherlands): Springer Science + Business Media. 2014; 369–431.
33. UniProtKB. 2017. <http://www.uniprot.org/uniprot/>.
34. Howard S, Amin N, Benowitz AB, Chiarparin E, Cui H, Deng X, et al. Fragment-based discovery of 6-azaindazoles as inhibitors of bacterial DNA ligase. *ACS Med Chem Lett.* 2013;4:1208–12.
35. Streker K, Schäfer T, Freiberg C, Brötz-Oesterhelt H, Hacker J, Labischinski H, et al. In vitro and in vivo validation of ligA and tarI as essential targets in *Staphylococcus aureus*. *Antimicrob Agents Chemother.* 2008;52:4470–74.
36. Small-Molecule Drug Discovery Suite 2017-1, New York: Schrödinger, Inc.; 2017. <https://www.schrodinger.com/citations>.
37. Harder E, Damm W, Maple J, Wu C, Reboul M, Xiang JY, et al. OPLS3: a force field providing broad coverage of drug-like small molecules and proteins. *J Chem Theory Comput.* 2016;12:281–96.
38. Surivet JP, et al. Structure-guided design, synthesis and biological evaluation of novel DNA ligase inhibitors with in vitro and in vivo anti-staphylococcal activity. *Bioorg Med Chem Lett.* 2012;22: 6705–11.
39. Friesner RA, Murphy RB, Repasky MP, Frye LL, Greenwood JR, Halgren TA, et al. Extra precision glide: docking and scoring incorporating a model of hydrophobic enclosure for protein–ligand complexes. *J Med Chem.* 2006;49:6177–96.
40. Stokes SS, Gowravaram M, Huynh H, Lu M, Mullen GB, Chen B, et al. Discovery of bacterial NAD⁺-dependent DNA ligase inhibitors: improvements in clearance of adenosine series. *Bioorg Med Chem Lett.* 2012;22:85–9.
41. Ludlow RF, Verdonk ML, Saini HK, Tickle IJ, Jhoti H. Detection of secondary binding sites in proteins using fragment screening. *PNAS.* 2015;112:15910–5.
42. Tian W, Chen C, Lei X, Zhao J, Liang J. CASTp 3.0: computed atlas of surface topography of proteins. *Nucleic Acids Res.* 2018;46:W363–W367. <https://doi.org/10.1093/nar/gky473>.